

Universality and Final Spin in Eccentric Binary Black Hole Inspirals

Ian Hinder, Birjoo Vaishnav, Frank Herrmann, Deirdre M. Shoemaker, and Pablo Laguna
Center for Gravitational Wave Physics, The Pennsylvania State University, University Park, PA 16802

We present results from numerical relativity simulations of equal mass, non-spinning binary black hole inspirals and mergers with initial eccentricities $e \leq 0.8$ and coordinate separations $D \geq 12 M$ of up to 9 orbits (18 gravitational wave cycles). We extract the mass M_f and spin a_f of the final black hole and find, for eccentricities $e \lesssim 0.4$, that $a_f/M_f \approx 0.69$ and $M_f/M_{\text{adm}} \approx 0.96$ are independent of the initial eccentricity, suggesting that the binary has circularized by the merger time. For $e \gtrsim 0.5$, the black holes plunge rather than orbit, and we obtain a maximum spin parameter $a_f/M_f \approx 0.72$ around $e = 0.5$. In addition, we observe that for $e \lesssim 0.4$ the binary enters, at $t \sim 50 M_f$ before the amplitude of the gravitational radiation peaks, a *universal* plunge previously only observed in circular binary black hole inspirals.

The field of numerical relativity (NR) has now entered a stage where binary black hole (BBH) simulations can reliably be used to investigate a vast range of interesting phenomena. Studies have produced gravitational waveforms from binary systems in essentially circular orbits [1, 2, 3, 4], involving spinning black holes as well as unequal mass systems. The level of numerical accuracy achieved by these codes is impressive [4, 5], and in some of these studies, the initial binary separations were such that it was feasible to directly compare with post-Newtonian (PN) waveforms [3, 4]. Other examples of exciting new results in NR are investigations of the kick imparted to the final black hole (BH) [6, 7, 8], the spin dynamics of the merging BHs [9, 10], and, of relevance to the present work, the merger threshold between bound and unbound BBHs [11, 12]. All of this has been possible since the pioneering work of Brüggmann et al. [13], Pretorius [14], Baker et al. [15], Campanelli et al. [16].

It is well known that gravitational radiation leads to circularization of a binary system [17]. In this work, we study this circularization in the nonlinear regime and investigate connections with the results by Baker et al. [1]. In Ref. [1], it was found that, for equal-mass, non-spinning BHs initially in quasi-circular orbits, the merger produced a BH with spin parameter $a_f/M_f \sim 0.69$, which, within the accuracy of the results, was independent of the initial separation. Another finding was that, at $t \sim 50 M_f$ before the amplitude of the gravitational wave reaches its peak, the BBHs enter a *universal* plunge during which the binary has lost “memory” of its initial conditions.

In this *Letter*, our main goals are (1) to investigate whether sufficient eccentricity is lost during the late stages of inspiral to circularize the orbit and exhibit the same *universality* as in the circular case and (2) to extract the spin parameter and mass of the final BH, and compare the values with those from circular inspirals.

Although isolated stellar mass BBHs will have completely circularized by the time they are observable by ground-based interferometers, scenarios have been suggested for which BBHs in eccentric orbits are not only astrophysically interesting but also could be detected by space- or ground-based interferometers [18, 19]. For instance, galactic mergers leave behind massive BBHs that

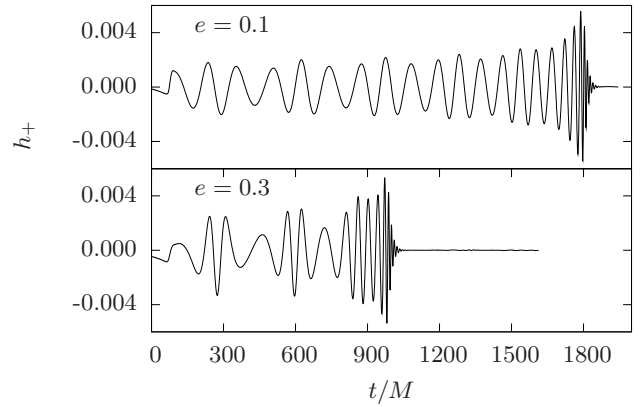


FIG. 1: Waveform polarizations h_+ for the cases $e = 0.1$ (top) and $e = 0.3$ (bottom) extracted at $r = 70M$.

likely interact with a gaseous environment. A gaseous-gravitational driven inspiral could yield a BBH arriving at the last few orbits and merger with a non-vanishing eccentricity. An observation of the gravitational waves from an eccentric BBH merger will allow us to determine the amount of angular momentum lost to gas and, in particular, the gravitational torques between the binary and a circumbinary disc that affect the eccentricity of the binary [20].

The implications of eccentricity in the merger part of waveforms when searching for and characterizing BBH signals needs to be fully investigated. Figure 1 shows two examples of waveforms from orbits with eccentricity $e = 0.1$ (top) and $e = 0.3$ (bottom). There are evident differences in the two waveforms. The higher eccentricity waveform shows fewer gravitational wave cycles and stronger modulations in the chirp signal. However, once the signal reaches the plunge and ringdown phase, there seems to be a *universal* behavior which may have interesting consequences in the parameter estimation from ringdown waveforms.

We construct initial data using the puncture approach [21], which requires specifying the coordinate lo-

e	D/M	$P_{1,2}/M$	$m_{1,2}/M$	M_{adm}/M	J_{adm}/M^2
0.00	12.000	0.0850	0.4883	0.991122	1.0200
0.05	12.832	0.0792	0.4891	0.991049	1.0163
0.10	13.645	0.0741	0.4898	0.991043	1.0111
0.15	14.456	0.0695	0.4904	0.991036	1.0047
0.20	15.264	0.0651	0.4910	0.991029	0.9937
0.30	16.870	0.0571	0.4920	0.991012	0.9633
0.40	18.459	0.0498	0.4928	0.990990	0.9193
0.50	20.023	0.0429	0.4934	0.990959	0.8590
0.60	21.539	0.0361	0.4940	0.990909	0.7776
0.70	22.955	0.0292	0.4944	0.990822	0.6703
0.80	24.072	0.0214	0.4948	0.990625	0.5151

TABLE I: *Initial data parameters*: The runs are labeled by their initial eccentricity e . The punctures have bare masses $m_{1,2}/M$, linear momenta $\pm P_{1,2}/M$, and are separated by a distance D/M . The ADM masses and angular momenta of the spacetimes are given by M_{adm} and J_{adm}

cations and momenta for the two BHs. For “circular” orbits, we follow [22]. For eccentric models, we use the conservative 3PN expressions in Ref. [23]. These expressions require the specification of the eccentricity e (of the three PN eccentricities, we choose e_t) and the mean motion $n = 2\pi/P_r$, where P_r is the radial (pericenter to pericenter) orbital period. It is important to keep in mind that the eccentricities we quote (and we use them also to label the models) are to be taken only as a guide to the eccentricity in the initial data, as the PN expressions used do not include radiation reaction, and the PN parameters are in a different coordinate system to the puncture initial data.

We construct a family of initial data by fixing $n = 0.01625/M$ ($P_r \sim 387M$) and varying e in the range $0.05 - 0.8$ (note that to 2PN order, this means that the systems have the same binding energy and that, at high eccentricities, there are portions of the orbit for which the PN condition $v/c \ll 1$ is no longer valid). The binary separation D is determined from Eq. (23) in Ref. [23], and the tangential linear momentum, P/M , of each BH at apocenter is obtained from $J = PD$, where J is the total angular momentum computed as a PN expansion in n and e (Eq. (21) in Ref. [23]). The bare BH masses $m_{1,2}$ are chosen to make the irreducible BH masses $M_{1,2} = 0.5$ (i.e. $M = M_1 + M_2 = 1$). Table I provides the initial data parameters.

The numerical simulations and results in this work were obtained with the same infrastructure [24, 25, 26, 27] used in our previous BBH studies [7, 10, 28, 29]. We have evolved the circular model at three different resolutions (finest grid spacings of $M/38.7$, $M/51.6$ and $M/64.5$). We obtain approximately fourth order convergence in the total energy and angular momentum radiated, consistent with the designed 4th order accuracy.

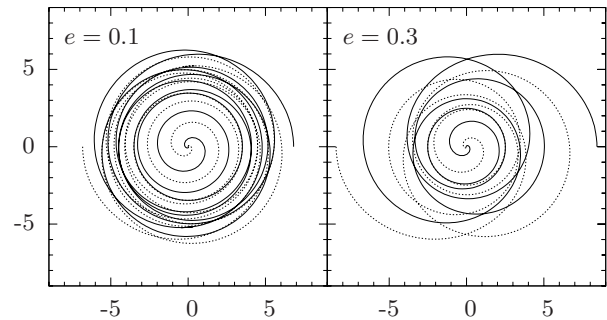


FIG. 2: Inspiral tracks for initial eccentricity $e = 0.1$ (left panel) and $e = 0.3$ (right panel).

The eccentric simulations are all performed utilizing both symmetries $z \mapsto -z$ and $\phi \mapsto \phi + \pi$ with a finest grid spacing of $M/38.7$. The high resolution circular run consumed just under 10000 CPU hours over 12 days, evolving roughly $8M/hr$ during the inspiral phase. The eccentric runs, at lower resolution, took a total of about 7000 CPU hours and were typically run on 8–16 processors evolving roughly $20 M/hr$ during the inspiral.

In Fig. 2, we display the coordinate inspiral tracks for $e = 0.1$ (left) and $e = 0.3$ (right). It is evident that the difference in initial eccentricity has a large effect during the inspiral. Qualitatively, the case with larger eccentricity exhibits a more rapid inspiral[17]. However, at some point both systems enter a “circular” plunge, hinting that circularization may have occurred. We find that the simulations with $e \geq 0.5$ show plunge-type rather than orbital-type behavior in the coordinate motion from the very start. A word of caution is needed. The tracks shown in Fig. 2 represent the coordinate positions of the individual BHs, and once a common horizon forms, they are less meaningful.

We now consider the emitted radiation and focus on the dominant $\ell = 2, m = 2$ mode of the complex Newman-Penrose (NP) quantity $\Psi_4 = A(t) \exp(-i\varphi(t))$. To compare the orbits, we apply a time shift to A and φ as in Ref. [1], so the maximum of A (i.e. the peak of the amplitude of the gravitational wave) is at $t/M_f = 0$ in each evolution. In Fig. 3, we plot the shifted amplitudes and frequencies $\omega = d\varphi/dt$ extracted at $r = 70M$. The cases displayed are those with eccentricities $e = 0 - 0.5$ in steps of 0.1 and $e = 0.8$.

In Fig. 3, the oscillations and growth in A and ω at early times (inspiral) can be in general terms understood from simple Newtonian considerations [17]. That is, ignoring radiation reaction, the oscillations (i.e. amplitude and period) in A and ω are a direct consequence of the eccentricity and not present in the $e = 0$ case. The period of these oscillations is the period P_r of the extrema

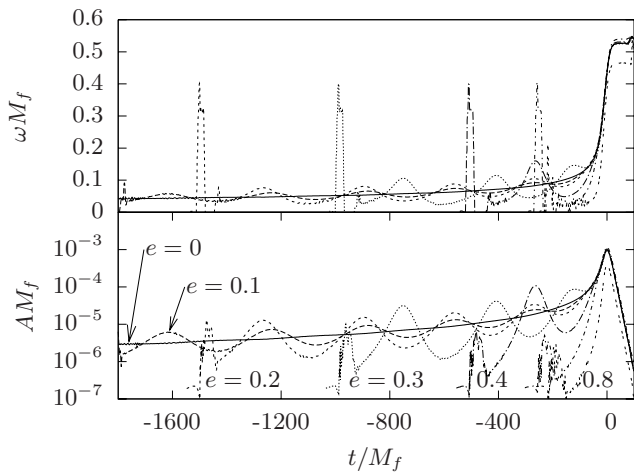


FIG. 3: Frequency and amplitude of the $\ell = 2$, $m = 2$ mode of the NP radiation scalar $r\Psi_4$ extracted at $r = 70 M$. The cases displayed are those with eccentricities $e = 0 - 0.5$ in steps of 0.1 and $e = 0.8$ which does not show the universal behavior.

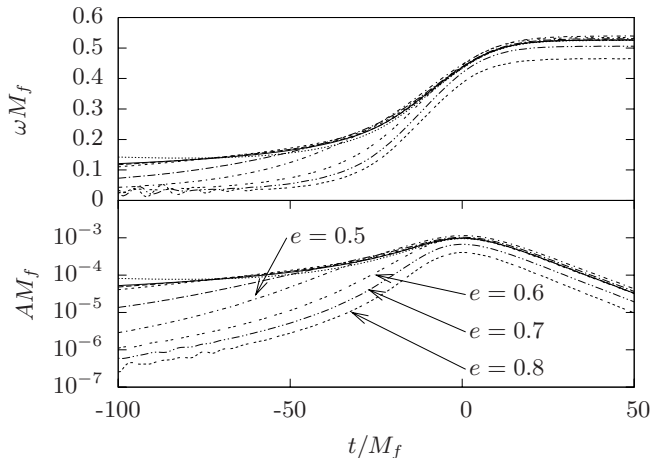


FIG. 4: As in Fig.3 but focusing on the region just before the peak of the amplitude of the gravitational wave. Here we plot eccentricities $e = 0 - 0.8$ in steps of 0.1.

in the separation, and the amplitude of the oscillations increases with e . If one adds radiation reaction, the amplitude of the oscillations in A and ω damps and their period shortens, corresponding to a reduction in eccentricity. As expected, there is in addition an overall growth of A and ω due to the energy and angular momentum loss. Also consistent with the predictions in [17], the higher eccentricity evolutions merge more quickly. We note that in the Newtonian case, we would observe that $P_r = P_\phi$, where P_ϕ is the time the binary takes to complete one revolution in the angular coordinate ϕ . Due to the effects of precession caused by GR, the two periods are very different (this can be seen from PN equations).

During the merger or plunge phase, both A and ω increase dramatically until A reaches a maximum and ω

levels off, signaling that the BBH has already merged. After this point, A decays exponentially and ω remains constant, a direct consequence of the quasi-normal mode (QNM) ringing of the final BH. The spikes observed in Fig. 3 at the beginning of each run are due to a small amount of spurious radiation present in the initial data. Finally, one can clearly see that the $e = 0.7$ and 0.8 case are basically plunging.

As mentioned before, one of the objectives of this work is to investigate whether a given initial data configuration will circularize before it merges. By this we mean that the radiation from the late stages of the evolution is identical to that from an orbit which started with zero eccentricity. We see in Fig. 3 indications that the low e evolutions show the *universality* of a circular orbit at the very late stage of inspiral. Both A and ω near $t/M_f \approx 0$ seem to be indistinguishable for low enough eccentricity. In order to investigate this in more detail, in Fig. 4 we focus on the plunge stage. Here we plot eccentricities $e = 0 - 0.8$ in steps of 0.1. Up until $e = 0.4$ and after $t/M_f \approx -50$, the amplitudes A from each run follow each other, similarly with ω . Noticeable differences start showing for $e \geq 0.5$, which is the first configuration to plunge immediately without orbiting first.

We now discuss M_f and a_f , computed using two independent methods. In one method, they are obtained from the radiated energy and angular momentum using $M_f = M_{\text{adm}} - E_{\text{rad}}$ and $a_f/M_f = (J_{\text{adm}} - J_{\text{rad}})/M_f^2$. In the second method, M_f and a_f are computed from the QNM frequencies emitted by the final BH following Ref. [30]. As a cross-check, for some of the models we also determine a_f/M_f using an approximate technique derived from the isolated horizon formalism [10, 31]. Table II gives the energy E_{rad} and angular momentum J_{rad} radiated as well as the final mass M_f and spin a_f . In order to help understand the results, we also display M_f and spin a_f in Fig. 5 as a function of e . Notice the agreement in a_f and M_f that the three methods give within the estimated error bars.

Given an initial eccentricity, it is possible to choose a large enough semimajor axis or orbital period for which the binary circularizes when it arrives at the merger. Our family of initial configurations was designed to investigate, for a fixed initial orbital period, how much initial eccentricity a binary is able to have and still enter the merger with essentially vanishing eccentricity. Since we do not have a good measure of eccentricity applicable prior to the merger, we focus on the end state, namely M_f and a_f of the final BH. We see from Fig. 5 that $a_f/M_f \approx 0.69$ for $e \lesssim 0.4$ and $M_f/M_{\text{adm}} \approx 0.96$ for $e \lesssim 0.5$, both values of M_f and a_f in agreement with the circular result. We note that the remaining orbits, the ones which do not circularize, are all configurations which seem to plunge immediately rather than entering an orbital phase. We conclude that for the systems we studied with approximately constant initial orbital period, within our error bars, orbits with $e \lesssim 0.4$ essentially circularize before they merge, and orbits with $e \gtrsim 0.5$ plunge.

e	$\frac{E_{\text{rad}}}{M_{\text{adm}}}$	$\frac{J_{\text{rad}}}{M_{\text{adm}}^2}$	$\frac{a_f}{M_f} _{\text{rad}}$	$\frac{a_f}{M_f} _{\text{qnm}}$	$\frac{a_f}{M_f} _{\text{ih}}$	$\frac{M_f}{M_{\text{adm}}} _{\text{rad}}$	$\frac{M_f}{M_{\text{adm}}} _{\text{qnm}}$
0.00	0.039	0.391	0.714	0.689	—	0.961	0.964
0.05	0.039	0.388	0.713	0.688	—	0.961	0.963
0.10	0.040	0.388	0.707	0.689	—	0.960	0.963
0.15	0.039	0.385	0.696	0.690	—	0.961	0.964
0.20	0.040	0.389	0.676	0.690	—	0.960	0.963
0.30	0.039	0.372	0.686	0.686	0.681	0.961	0.964
0.40	0.040	0.279	0.716	0.698	0.693	0.960	0.962
0.50	0.038	0.190	0.742	0.717	0.712	0.962	0.964
0.60	0.022	0.108	0.713	0.707	0.702	0.978	0.980
0.70	0.011	0.063	0.623	0.641	0.634	0.989	0.994
0.80	0.004	0.033	0.484	0.515	0.502	0.996	1.002

TABLE II: *Extracted quantities:* Energy E_{rad} and angular momentum J_{rad} radiated; final spin parameter a_f and mass M_f computed from J_{rad} and E_{rad} as well as from QNM ring-

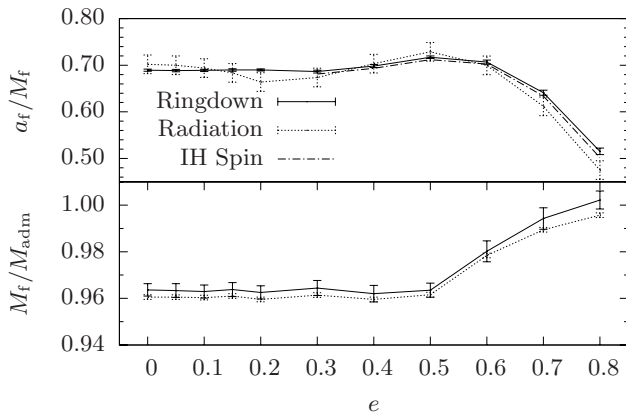


FIG. 5: Plots of M_f/M_{adm} and a_f/M_f as functions of the initial eccentricity e from Table II. Note that the error bars shown here on the radiation quantities for eccentric runs are copied from the $e = 0$ case and thus should be treated as indicative only.

We also observe for $e \gtrsim 0.4$ that rather than a_f decreasing monotonically, a maximum spin parameter $a_f/M_f \approx 0.72$ is obtained around $e = 0.5$. Given the size of our

uncertainties and that the maximum is found in the two independent methods used to calculate the spin, we are confident that this maximum is real for our family of initial data. At about $e = 0.6$, a_f starts decreasing monotonically. We are currently considering larger, but still computationally feasible, initial separations to investigate if there is *any* bound orbital (rather than plunge) configuration that does not circularize.

As $e \rightarrow 1$, corresponding to vanishing linear momenta (i.e. a head-on collision from rest), we find that $a_f/M_f \rightarrow 0$, in line with the symmetry of the head-on collision, and $M_f \sim M_{\text{adm}}$, as expected, since NR simulations of a head-on collision have shown that $M_f \sim (1 - 0.001)M_{\text{adm}}$ [32].

In summary, we have carried out a series of eccentric orbit simulations of BBH systems in full nonlinear GR to investigate the merger regime and final BH. The family of simulations consisted of binaries with approximately constant initial orbital period and varying initial eccentricity. We found that for initial $e \leq 0.4$, the final BH parameters are $M_f/M_{\text{adm}} \approx 0.96$ and $a_f/M_f \approx 0.69$, the same as in the circular case. We also find that for $e \leq 0.4$ the binary begins to enter a *universal* plunge at $t \sim 50 M_f$ before the amplitude of the gravitational radiation reaches its peak, as observed in the circular case. In a sense, one effect is a consequence of the other. Namely, the emergence of a *universal* plunge implies that the final state of the system, i.e. the final BH, is “unique.” Reaching the same final state is also a strong indication that the binary has circularized by the time it enters the plunge.

While preparing the manuscript of this work, a study by Sperhake et al. [33] appeared with both similar and complementary conclusions to those in our present work.

Acknowledgments

This work was supported in part by NSF grants PHY-0354821, PHY-0653443, PHY-0244788, PHY-0555436 and PHY-0114375 (CGWP). Computations were performed at NCSA and TACC under allocation TG-PHY060013N. The authors thank M. Ansorg, E. Bentivegna, T. Bode, A. Knapp, R. Matzner and E. Schnetter for contributions to the computational infrastructure and helpful discussions, and E. Berti for the data tables used in the quasinormal fitting.

[1] J. G. Baker, J. Centrella, D.-I. Choi, M. Koppitz, and J. van Meter, Phys. Rev. **D73**, 104002 (2006).
[2] M. Campanelli, C. O. Lousto, Y. Zlochower, and D. Merritt, Ap. J. Lett. **659**, L5 (2007).
[3] M. Hannam, S. Husa, U. Sperhake, B. Bruggmann, and J. A. Gonzalez, preprint (arXiv:0706.1305) (2007).
[4] M. Boyle, D. A. Brown, L. E. Kidder, A. H. Mroue, H. P. Pfeiffer, M. A. Scheel, G. B. Cook, and S. A. Teukolsky,

preprint (arXiv.org:0710.0158) (2007).
[5] S. Husa, J. A. Gonzalez, M. Hannam, B. Bruegmann, and U. Sperhake, preprint (arXiv.org:0706.0740) (2007).
[6] J. A. Gonzalez, U. Sperhake, B. Bruegmann, M. Hannam, and S. Husa, Phys. Rev. Lett. **98**, 091101 (2007).
[7] F. Herrmann, I. Hinder, D. Shoemaker, P. Laguna, and R. A. Matzner, Astrophys J. **661**, 430 (2007).
[8] J. G. Baker, J. Centrella, D.-I. Choi, M. Koppitz, J. R.

- van Meter, and M. C. Miller, *Ap. J. Lett.* **653**, L93 (2006).
- [9] M. Campanelli, C. O. Lousto, and Y. Zlochower, *Phys. Rev. D* **74**, 041501 (2006).
- [10] F. Herrmann, I. Hinder, D. M. Shoemaker, P. Laguna, and R. A. Matzner, preprint (arXiv:0706.2541) (2007).
- [11] F. Pretorius, *Class. Quant. Grav.* **23**, S529 (2006).
- [12] F. Pretorius and D. Khurana, preprint (gr-qc/0702084) (2007).
- [13] B. Brügmann, W. Tichy, and N. Jansen, *Phys. Rev. Lett.* **92**, 211101 (2004).
- [14] F. Pretorius, *Phys. Rev. Lett.* **95**, 121101 (2005).
- [15] J. G. Baker, J. Centrella, D.-I. Choi, M. Koppitz, and J. van Meter, *Phys. Rev. Lett.* **96**, 111102 (2006).
- [16] M. Campanelli, C. O. Lousto, P. Marronetti, and Y. Zlochower, *Phys. Rev. Lett.* **96**, 111101 (2006).
- [17] P. C. Peters, *Phys. Rev.* **136**, B1224 (1964).
- [18] M. C. Miller and D. P. Hamilton, *Astrophys. J.* **576**, 894 (2002).
- [19] L. Wen, *Astrophys. J.* **598**, 419 (2003).
- [20] P. J. Armitage and P. Natarajan, *Astrophys. J.* **634**, 921 (2005).
- [21] P. Anninos, R. H. Price, J. Pullin, E. Seidel, and W.-M. Suen, *Phys. Rev. D* **52**, 4462 (1995).
- [22] S. Husa, M. Hannam, J. A. Gonzalez, U. Sperhake, and B. Brügmann, preprint (arXiv:0706.0904) (2007).
- [23] C. Königsdörffer and A. Gopakumar, *Phys. Rev. D* **73**, 124012 (2006).
- [24] Cactus, <http://www.cactuscode.org> (2007).
- [25] E. Schnetter, S. H. Hawley, and I. Hawke, *Class. Quant. Grav.* **21**, 1465 (2004).
- [26] S. Husa, I. Hinder, and C. Lechner, *Computer Physics Communications* **174**, 983 (2006).
- [27] M. Ansorg, B. Brügmann, and W. Tichy, *Phys. Rev. D* **70**, 064011 (2004).
- [28] F. Herrmann, I. Hinder, D. Shoemaker, and P. Laguna, *Class. Quant. Grav.* **24**, S33 (2007).
- [29] B. Vaishnav, I. Hinder, F. Herrmann, and D. Shoemaker, *Phys. Rev. D* **76**, 084020 (2007).
- [30] E. Berti, V. Cardoso, J. A. González, and U. Sperhake, *Phys. Rev. D* **75**, 124017 (2007).
- [31] A. Ashtekar and B. Krishnan, *Living Rev. Rel.* **7**, 10 (2004).
- [32] P. Anninos, D. Hobill, E. Seidel, L. Smarr, and W.-M. Suen, *Phys. Rev. Lett.* **71**, 2851 (1993).
- [33] U. Sperhake, E. Berti, V. Cardoso, J. Gonzalez, B. Brügmann, and M. Ansorg, preprint (arXiv:0710.3823) (2007).